



Shahrood University of
Technology



Iranian Society of
Mining Engineering
(IRSM)

Structural Controls on Orogenic Gold Mineralization in High-Grade Metamorphic Rocks: Insights from the Nathenje Prospect, Central Malawi

Joshua Chisambi^{1*}, Leornard Kalindekafe², Kettie Magwaza², Ruth Mumba² and Martin Kameza²

1. Department of Mining Engineering, Malawi University of Business and Applied Sciences: Blantyre, Malawi

2. Malawi Mining Investment Company (MAMICO), Lilongwe, Malawi

Article Info

Received 5 June 2025

Received in Revised form 30 July 2025

Accepted 29 August 2025

Published online 29 August 2025

DOI: [10.22044/jme.2025.16348.3183](https://doi.org/10.22044/jme.2025.16348.3183)

Keywords

Orogenic gold

Structural control

Shear zones

Fold hinges

Malawi Basement Complex

Abstract

The Nathenje region in central Malawi hosts significant gold mineralization within high-grade metamorphic rocks of the Mozambique Belt, yet remains underexplored despite extensive artisanal mining activity. The structural controls on primary bedrock gold mineralization within these high-grade metamorphic rocks remain poorly understood, limiting systematic exploration and resource development. We conducted integrated field mapping, structural analysis, petrographic examination, and geochemical sampling to characterize gold mineralization controls in the Nathenje prospect, central Malawi. Detailed structural measurements combined with stereographic analysis reveal three deformation phases, with gold mineralization predominantly associated with D₂ transpressional structures. Fire assay results demonstrate significant gold concentrations (0.15–5.0 g/t Au) in arsenopyrite-bearing quartz veins, with the highest grades systematically occurring at structural complexity zones. Petrographic analysis reveals native gold particles (5–50 μm) intimately associated with arsenopyrite along grain boundaries and within microfractures, indicating coupled precipitation processes. Critically, we identify a hierarchical structural control system operating from regional NE-SW trending shear zones to microscale sulphide boundaries, with fold hinges, dilutional jogs, and amphibolite-gneiss contacts yielding consistently higher gold grades (>3 g/t Au) than other structural settings. Our results establish the first comprehensive structural model for gold mineralization in central Malawi's metamorphic terrain and provide specific targeting criteria applicable to similar high-grade metamorphic environments throughout the East African Orogen.

1. Introduction

Malawi's geology is dominated by high-grade metamorphic rocks of the Mozambique Belt, yet the country has not seen the systematic gold exploration or production documented in neighbouring Tanzania, Mozambique, and Zimbabwe [1]. Gold mining in Malawi has traditionally been restricted to artisanal and small-scale activities targeting alluvial and eluvial deposits, with limited characterization of primary bedrock sources [2], [3], [4]. The Nathenje area in central Malawi has emerged as a significant focus of artisanal gold mining, with local miners successfully extracting gold from stream

sediments. However, the geological controls on the primary mineralization feeding these secondary deposits remain poorly understood.

Early studies confirmed the presence of alluvial gold in southern and central Malawi but emphasized the lack of geological data required to identify and assess hard-rock sources [5], [6]. More recent work by [2], [3], [4], [7], [8], [9] in the Kirk Range demonstrated the presence of shear-hosted gold mineralization metamorphic rocks within NE-SW trending ductile shear zones, establishing an initial structural framework for primary gold in the region. This work highlighted the association of



gold with sulphide-bearing quartz-carbonate veins emplaced during Pan-African tectono-thermal events, raising important questions about the specific controls on mineralization and their potential regional significance.

The scarcity of detailed research on structural controls of gold mineralization in central Malawi represents a critical gap in our geological understanding. This gap has real consequences—limiting effective exploration and hindering development of Malawi's mineral sector. While artisanal miners successfully recover gold from streams around Nathenje, the primary bedrock sources and the geological structures controlling them remain poorly documented. Understanding these controls would not only guide more systematic exploration but would also contribute valuable insights to our knowledge of gold mineralization in high-grade metamorphic environments throughout the East African Orogen. This knowledge has practical significance for Malawi's economic development, as the mining sector currently contributes less than 1% to GDP despite the country's considerable geological potential [3], [9], [10], [11].

Our study addresses this knowledge gap by identifying and characterizing the key structural controls on gold mineralization in the Nathenje area. The results provide a comprehensive structural model for gold mineralization and establish specific targeting criteria that can guide future exploration efforts across Malawi's underexplored Precambrian terrain.

2. Geological Setting

Nathenje in Lilongwe is situated within the southern Mozambique Belt, which forms part of the East African Orogen, a major Neoproterozoic to early Palaeozoic orogenic system developed during the assembly of Gondwana [12]. The East African Orogen extends for approximately 6,000 km from Egypt in the north to Mozambique and Madagascar in the south, and represents the suture zone between East and West Gondwana [13], [14].

The Mozambique Belt, forming the southern portion of the East African Orogen, is characterized by high-grade metamorphic rocks that experienced intense deformation and metamorphism during the Pan-African Orogeny (ca. 650-500 Ma). In Malawi, the Mozambique Belt is dominated by amphibolite to granulite facies gneisses, schists, amphibolites, and marbles, with variable degrees of migmatization (Bloomfield. & Garson., 1965b). These rocks represent both reworked

Mesoproterozoic basement and Neoproterozoic supracrustal sequences.

Recent geochronological studies in Malawi and adjacent regions have revealed a complex tectono-metamorphic history for the Mozambique Belt, with multiple phases of deformation and metamorphism. U-Pb zircon dating has identified Mesoproterozoic protolith ages (1.2-1.0 Ga) for many of the orthogneisses, suggesting they represent reworked components of the Mesoproterozoic Irumide Belt [16], [17], [18], [19], [20], [21], [22]. The main Pan-African metamorphic events have been dated at circa 570-560 Ma (early high-pressure phase), 550-540 Ma (peak metamorphism), and 530-510 Ma (retrograde metamorphism and post-orogenic magmatism) [13].

The structural framework of the Mozambique Belt in Malawi is characterized by a dominant north-south to northeast-southwest structural grain, defined by major shear zones, foliation trends, and elongate granitoid plutons [18], [23]. These structures reflect the overall east-west to southeast-northwest compressional regime that dominated during the main phase of the Pan-African Orogeny. Figure 1 shows the regional geological map of the study area.

3. Methodology

This study employed an integrated approach combining detailed field mapping, structural analysis, and laboratory investigations to elucidate the controls on gold mineralization in the Nathenje area. The methodology was designed to systematically characterize the geological framework, with particular emphasis on structural elements and their relationship to mineralization patterns. Our approach incorporated both macroscopic field observations and microscopic analytical techniques to develop a comprehensive understanding of the mineralizing system across multiple scales.

3.1. Field Mapping and Structural Measurements

Geological mapping was conducted at a scale of 1:10,000, covering an area of approximately 5 km² centered on the Nathenje River and its tributaries—zones known for active artisanal gold panning. Systematic structural measurements were taken across exposed outcrops to characterize the orientation and kinematics of key features. Structural measurements were collected using a Brunton Geo Transit compass with magnetic

declination correction applied. The structural data were plotted on equal-area stereographic projections using Stereonet 10 software [24], [25] to identify dominant structural trends and patterns. Where preserved, kinematic indicators such as drag folds, vein boudinage, asymmetrical structures, and mineral lineations were carefully documented to infer the sense of movement and deformation history. Field observations systematically recorded

lithology (rock type, texture, mineralogy, and weathering), structural elements (foliation, lineation, joints, folds, and shear zones), quartz vein characteristics (morphology, size, orientation, and mineralogy), alteration features (type, intensity, and distribution), and evidence of mineralization (sulphides, iron oxides, and visual gold).

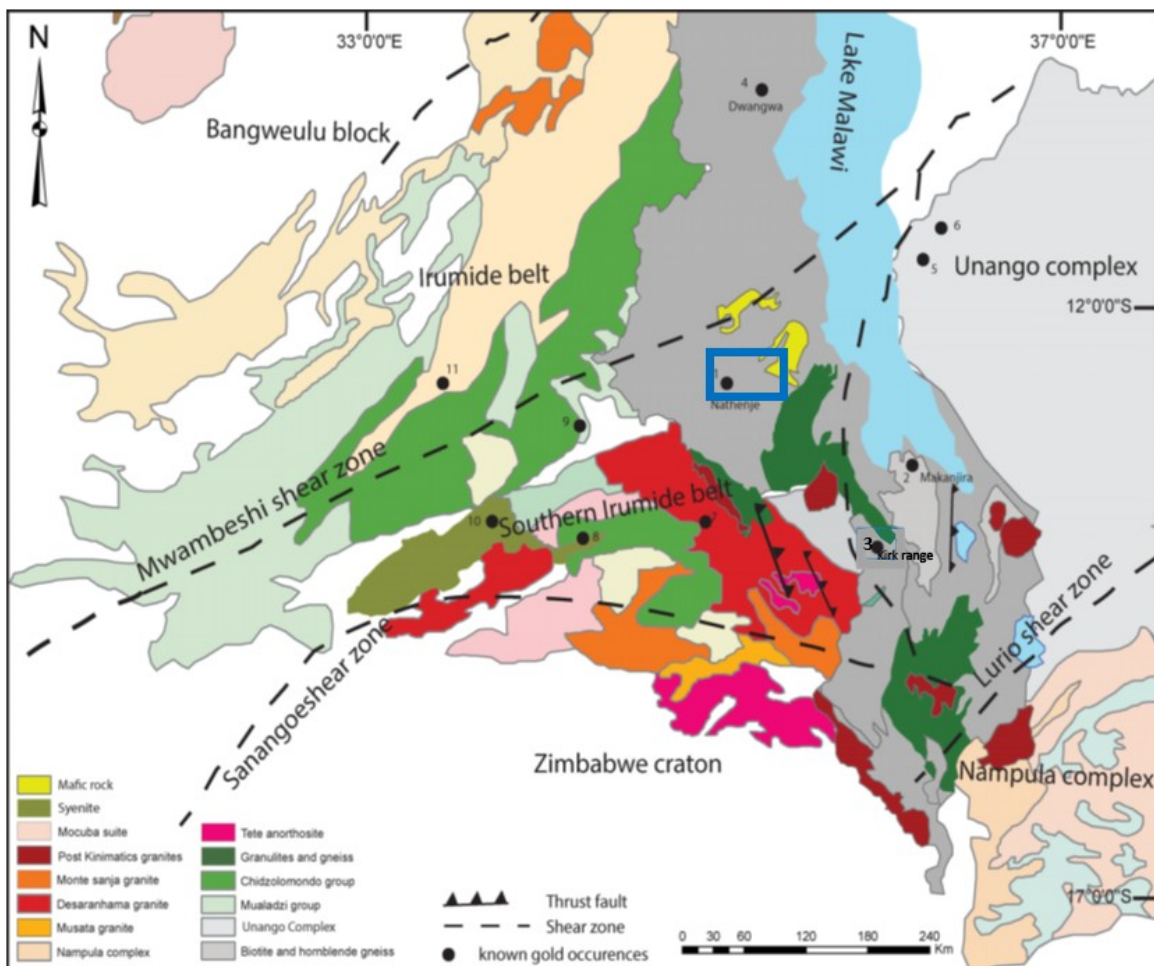


Figure 1. Modified after the authors in [2], showing the regional geological map of the study area. The map shows major tectonic domains, principal shear zones, and the distribution of high-grade metamorphic rocks.

3.2. Petrographic Analysis

Rock samples were collected from representative lithologies, including quartz veins, biotite gneisses, amphibolites, and visibly altered rocks. A total of 10 samples were collected. The study acknowledges that this sample size is limited, but in the scope of this work and due to field constraints, it offers a foundation for a larger sampling size.

Initial examination was performed in the field and laboratory using hand lenses and binocular

microscopes to assess texture, grain size, mineral assemblage, and evidence of sulphide mineralization. Five selected samples were processed into polished thin sections at the Malawi University of Business and Applied Sciences (MUBAS) Mining Engineering laboratory. The thin sections were analyzed under both transmitted and reflected light using an Olympus BX51 polarizing microscope equipped with a digital camera for photomicrography. Photomicrographs were taken of representative textures and mineral

associations, with particular emphasis on gold occurrences and their textural context.

3.2. Geochemical Analysis

Seven representative gold-bearing rock samples were selected for fire assay to quantify gold concentrations. The samples underwent a classic lead collection fire assay procedure at the Malawi University of Business and Applied Sciences (MUBAS) Mining Engineering laboratory. Quality control measures included the insertion of certified reference materials, blanks, and duplicates at a rate of 1 in 10 samples. The detection limit for the fire assay method was 0.01 g/t Au, with an analytical precision of $\pm 5\%$ for concentrations above 1 g/t Au.

These samples were strategically collected from different structural settings (fold hinges, shear zones, dilational jogs, and lithological contacts) to assess the correlation between gold grade and structural features.

4. Results and Discussions

We present the key findings from our integrated investigation. The results synthesize observations from field mapping, structural measurements, petrographic analysis, and geochemical data to establish the geological framework of gold mineralization in the study area.

4.1. Lithological Framework

The Nathenje area comprises high-grade metamorphic rocks of upper amphibolite to granulite facies, dominated by biotite gneiss with alternating quartz-feldspar and biotite-rich bands showing migmatitic textures in high-strain zones. Other units include competent amphibolite bands and lenses that control strain partitioning, resistant quartzo-feldspathic gneiss exhibiting less deformation, and thin, discontinuous garnetiferous schist occurring primarily at lithological boundaries.

The structural architecture exhibits a pronounced tectonic grain with all rock types displaying a steeply dipping NE-SW trending foliation. Structural mapping reveals a polydeformed basement terrane characterized by high-strain fabrics and complex fold geometries (Figure 2).

Structural mapping and analysis reveal three sequential deformation phases that have affected the Nathenje area. The earliest recognizable deformation produced isoclinal folding and a penetrative foliation (S_1) during initial crustal thickening associated with continent-continent

collision. While S_1 is largely transposed by later deformation, relict F_1 isoclinal folds are preserved as intrafolial structures within the dominant S_2 foliation. These early structures established the primary architectural framework of the area.

Continued compression generated prominent NE-SW trending structures and a pervasive S_2 foliation D_2 that constitutes the dominant fabric in the region. Stereographic analysis of foliation measurements ($n=58$) shows a strong clustering around $045^\circ/60^\circ\text{SE}$, reflecting this regional fabric (Figure 3). F_2 folds are typically tight to isoclinal with axes trending NW-SE and plunging moderately ($30^\circ\text{-}45^\circ$) to the northwest. The intensity of S_2 varies with lithology, being strongest in biotite gneiss and more weakly developed in quartzo-feldspathic gneiss.

The D_3 phase represents a shift to transpressional deformation, characterized by the development of N-S trending brittle-ductile shear zones. Kinematic indicators, including S-C fabrics, asymmetric porphyroclasts, and drag folds, indicate predominantly sinistral strike-slip to oblique-slip movement along these shear zones.

4.2. Quartz Vein Types, Sulphides, and Alteration

Three distinct generations of quartz veins have been identified in the Nathenje area, each with characteristic features:

Type 1 foliation-parallel veins (1-10 cm thick) appear as thin, whitish to translucent quartz bodies that follow the regional fabric of the host rocks. In hand specimens, these veins display a strained, slightly milky appearance with a pinched and stretched (boudinaged) structure resulting from post-placement deformation. They contain scattered small sulphide grains concentrated along foliation planes, with yellowish-brown iron staining commonly developing along fracture surfaces. These veins generally contain less sulphide mineralization compared to other vein types and represent the earliest stage of vein formation.

Type 2 shear zone-hosted veins (10-50 cm thick), These form more substantial bodies within NE-SW trending brittle-ductile shear zones. Hand specimens of these veins reveal diverse textures including massive quartz ranging from whitish to smoky gray with abundant dark sulphide patches, layered or banded appearances with alternating sulphide-rich and quartz-rich zones, and brecciated textures consisting of angular quartz fragments cemented by dark sulphide-rich material (Figure

4). The quartz in these veins frequently displays a darker gray coloration associated with higher sulphide content. Deformation features such as folded banding and fractured appearances provide evidence of syn-tectonic emplacement. These veins are particularly well-developed at dilational jogs, fold hinges, and lithological contacts within shear zones.

Type 3 late extensional veins comprise clean, white to milky quartz that cross-cuts earlier structures with sharp boundaries. In hand specimens, these veins show minimal sulphide content, little visible evidence of deformation, and a relatively uniform texture and appearance. They represent the latest stage of vein formation during the transition from transpressional to extensional tectonics.

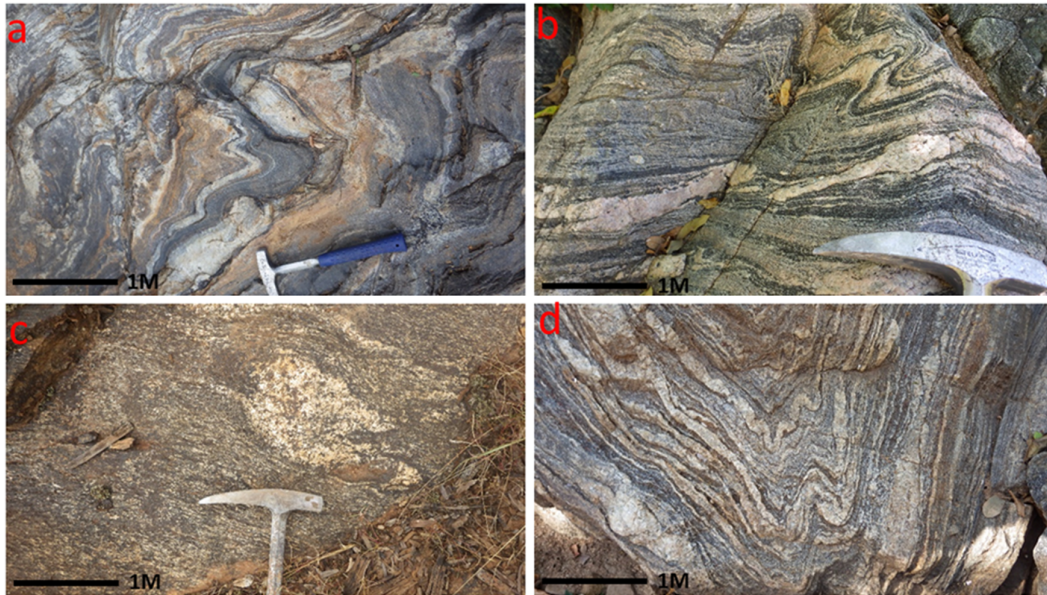


Figure 2: Field photographs illustrating key structural features associated with gold mineralization. (A) Isoclinal folding in banded biotite gneiss showing transposed foliation. (B) Sheath folding and asymmetric fold geometry in quartz-feldspar gneiss. (C) Quartz-feldspar segregation and strain concentration zones in high-grade gneiss. (D) F₂ fold interference patterns in migmatitic (ptygmatic) gneiss.

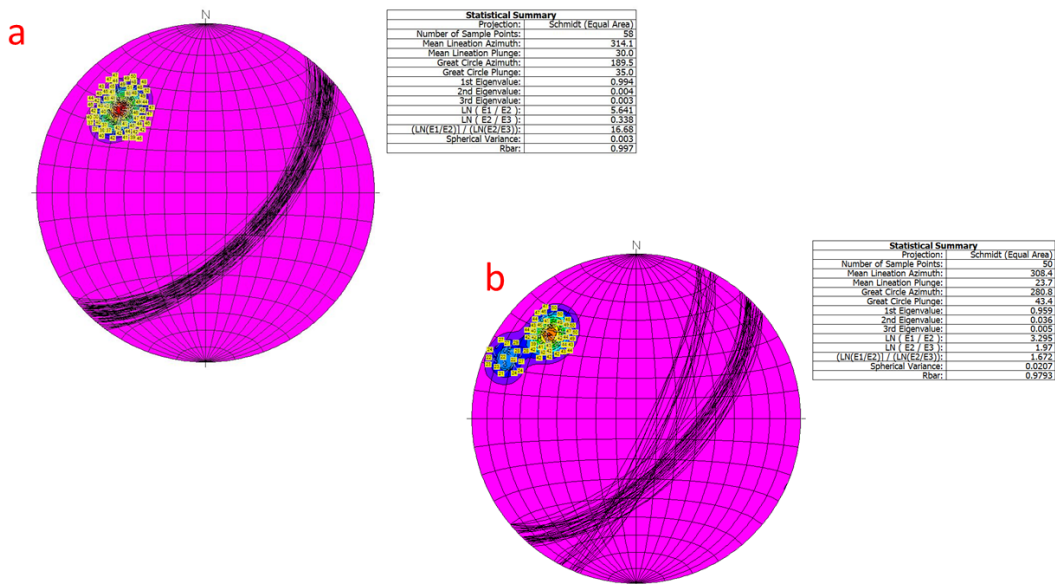


Figure 3. Stereographic projections of structural data from the Nathenje area. (A) Poles to foliation planes (n=58) showing a strong clustering around 045°/60°SE. (B) Poles to quartz vein orientations (n=50) showing two main clusters reflecting foliation-parallel and shear zone-hosted veins.

4.2.1. Sulphide Assemblages

The sulphide assemblage visible in hand specimens is dominated by brassy yellow pyrite occurring as either disseminated grains or clustered aggregates, particularly prominent in Type 2 veins (Figure 4). Some specimens contain golden-yellow chalcopyrite patches and steel-gray to bluish-gray arsenopyrite, creating distinctive dark metallic zones within the quartz. The distribution of these sulphides follows systematic patterns, with concentrated patches in structurally complex zones, alignment along visible deformation features, greater abundance in darker smoky quartz portions, and clustered accumulations at what appear to be fold hinges or dilational jogs.

Alteration features visible in hand specimens include prominent yellowish-brown to reddish-brown iron oxide staining (limonite/goethite) along fracture surfaces and surrounding sulphide minerals, representing weathering of primary sulphides and serving as a visual indicator of mineralized zones. The contact relationships

between veins and host rocks range from sharp to diffuse boundaries, with visible alteration halos indicated by colour changes in the adjacent rock. Notably, specimens showing vein contacts with amphibolite consistently display more intensive sulphide development than equivalent contacts with quartzo-feldspathic gneiss, suggesting a chemical influence on mineral precipitation in addition to structural controls. Quartz veins occur in two main orientations: dominantly parallel to foliation (040°-050°/55°-70°SE) and subordinately oblique to it (020°-030°/70°-85°SE) (Figure 3 b). Many of these veins display ductile deformation features including folding, boudinage, and shearing, suggesting emplacement during progressive deformation.

The presence of tight to isoclinal F_2 folds, Z-fold geometries, and sheath folds within the gneisses supports syn-tectonic mineralization. These structural features, created favourable conditions for strain localization and established critical pathways for mineralizing fluids.

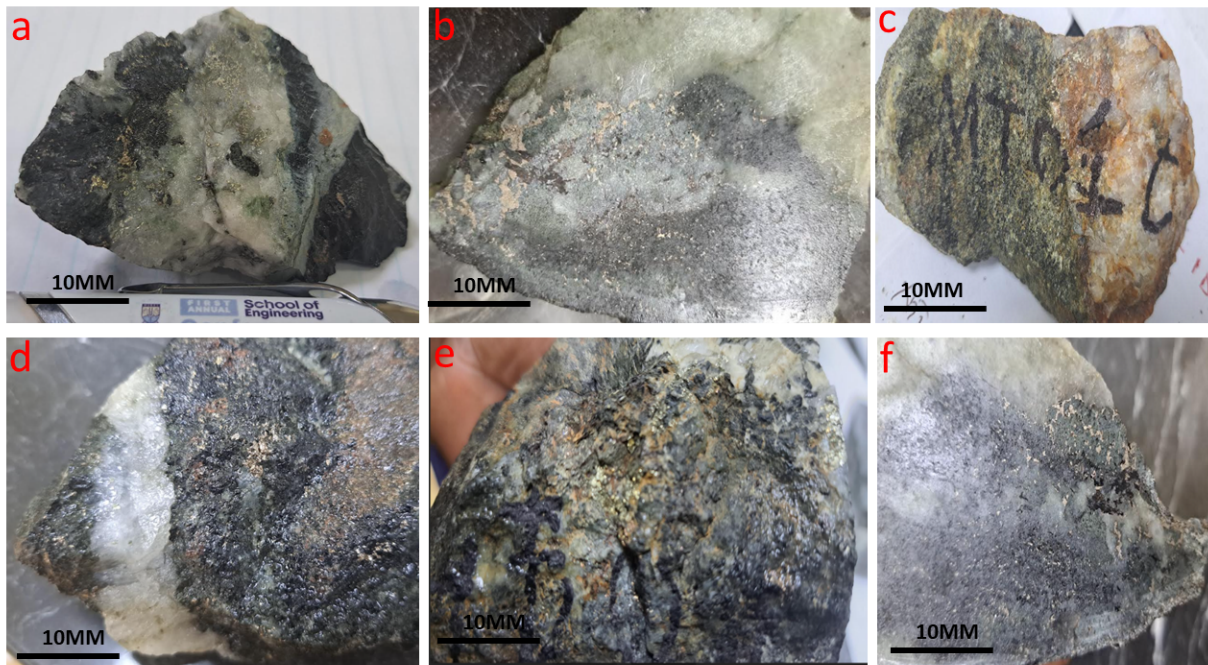


Figure 4. Photographs of representative hand specimens showing Type 2 shear zone-hosted quartz veins with characteristic sulphide mineralization. (a) Hand specimen exhibiting contrast between white to pale green quartz and dark sulphide-rich zones with visible metallic luster. (b) Close-up view showing contact between light-colored quartz and dense, dark metallic sulphide mineralization typical of pyrite-arsenopyrite assemblages. (c) Sample displaying prominent dark green to black sulphide-rich domains with gradational boundaries into lighter quartz-rich areas. (d) Specimen showing brecciated texture with angular fragments and contrast between white quartz and dark sulphide-rich zones. (e) Hand specimen exhibiting complex intergrowth of sulphide minerals with varied textures and some yellowish-brown iron oxide staining along fracture surfaces. (f) Sample

showing dense, fine-grained sulphide mineralization with characteristic dark metallic appearance and minor quartz veining

4.3. Gold Mineralization and Mineral Paragenesis

4.3.1. Gold Occurrence and Distribution

Gold mineralization in the Nathenje prospect is predominantly associated with sulphide assemblages hosted within quartz veins, particularly the Type 2 shear zone-hosted varieties. Reflected light microscopy reveals two primary modes of gold occurrence: visible native gold (Figure 5) and gold associated with arsenopyrite-bearing assemblages. Native gold occurs as discrete bright yellow particles (5-50 μm) with high reflectivity and characteristic morphology, distinguishing it from other metallic minerals present in the assemblage.

Detailed petrographic analysis demonstrates that gold exhibits systematic distribution patterns relative to host sulphides. Primary gold occurs as irregular grains intergrown with arsenopyrite and,

less commonly, with pyrite. The spatial association between arsenopyrite and gold is particularly pronounced, with gold particles frequently observed at arsenopyrite crystal boundaries or in fractures within arsenopyrite grains. This intimate relationship suggests a genetic link between arsenopyrite precipitation and gold deposition, consistent with observations from comparable orogenic gold systems worldwide [26], [27], [28], [29], [30].

The paragenetic sequence determined from crosscutting relationships observed in the study samples indicates that gold precipitation occurred during the main hydrothermal event associated with Type 2 vein emplacement. Microtextural evidence reveals gold deposition both synchronous with and slightly later than arsenopyrite formation, suggesting progressive evolution of mineralizing fluids during the main hydrothermal stage.

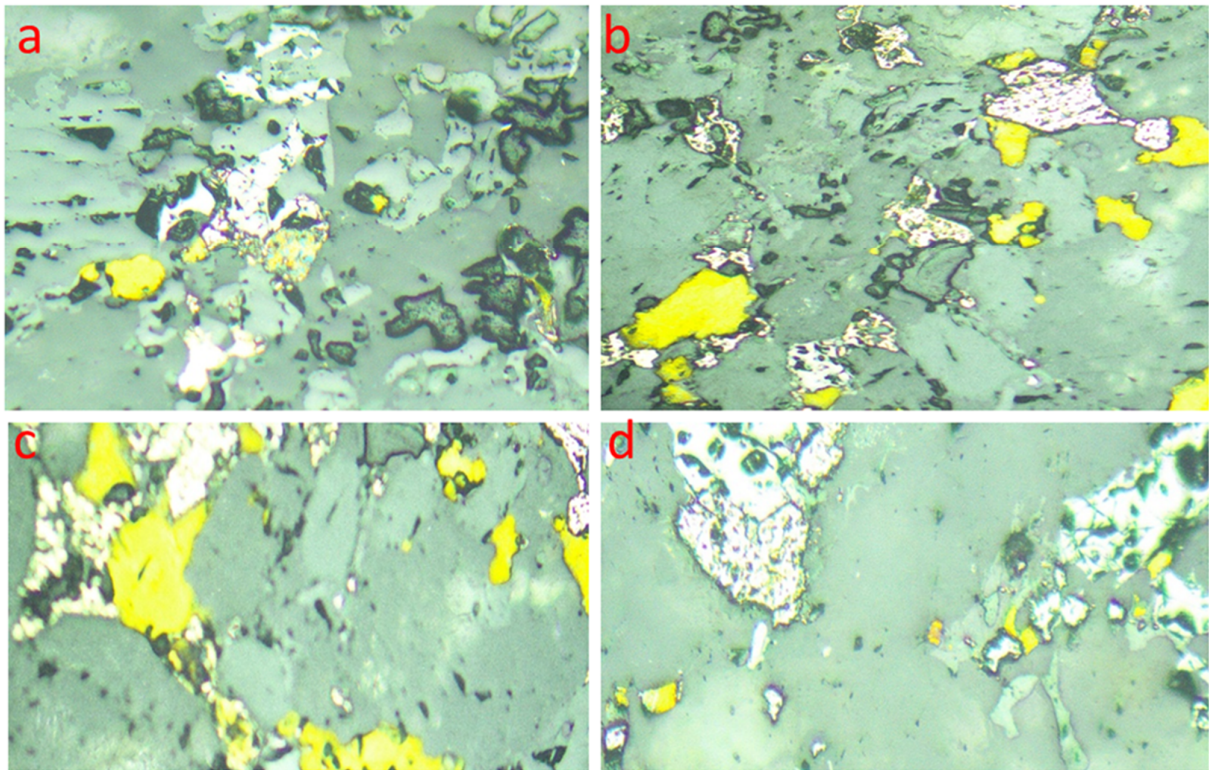


Figure 5. Gold mineralisation in yellow observed in thin sections

4.3.2. Mineral Paragenesis and Hydrothermal Evolution

The hydrothermal evolution and associated mineral paragenesis at Nathenje can be categorized

into three distinct stages based on microstructural relationships and overprinting criteria:

Stage I (Early Hydrothermal): Characterized by the formation of disseminated pyrite in altered wall rock and the development of

Type 1 foliation-parallel quartz veins with minor sulphide content. This stage predates the main gold mineralization event and likely corresponds to initial fluid infiltration along pre-existing structural anisotropies.

Stage II (Main Mineralization): The principal phase of economic mineralization, marked by the formation of arsenopyrite-rich assemblages and contemporaneous to slightly later precipitation of native gold. This stage corresponds to the development of Type 2 shear zone-hosted veins and features the most significant gold enrichment. The co-precipitation of arsenopyrite and gold suggests physicochemical conditions favouring simultaneous deposition, likely involving changes in sulphur fugacity, pH, or temperature during fluid-rock interaction.

Stage III (Late Hydrothermal): Represented by the formation of Type 3 extensional veins with minimal sulphide content and post-mineralization modification of earlier sulphide assemblages. This stage reflects the transition from transpressional to

extensional tectonics mentioned in the regional structural framework.

Textural analysis indicates that gold was primarily precipitated during Stage II, with gold grains showing a strong spatial affinity for arsenopyrite. This relationship suggests that arsenopyrite precipitation played a crucial role in triggering gold deposition, potentially through mechanisms such as electrochemical attraction, redox reactions at sulphide surfaces, or destabilization of gold-bearing aqueous complexes in response to changing fluid chemistry [31].

4.4. Geochemical Characteristics, Structural Controls, and Exploration Implications

4.4.1. Assay Results and Structural Controls

Fire assay analyses of selected rock samples from the Nathenje prospect confirm significant gold mineralization with concentrations ranging from 0.15 to 5.0 g/t Au (Table 1). The highest gold grades are consistently associated with sulphide-rich quartz veins located at zones of structural complexity, particularly fold hinges, dilational jogs, and lithological contacts.

Table 1. Gold fire assay results for selected rock samples from Nathenje area.

Sample ID	Rock Type	Au (g/t)	Description	Structural Setting
NTH-QV-01	Quartz Vein	0.84	Sheared quartz vein with pyrite along foliation	Shear zone
NTH-QV-02	Quartz Vein	4.2	Massive milky quartz with visible sulphides	Dilational jog
NTH-QV-03	Quartz Vein	2.11	Boudinaged vein in amphibolite	Foliation-parallel
NTH-HZR-01	Altered Host Rock	0.36	Sericite-chlorite altered schist	Vein margin
NTH-QV-04	Quartz Vein	5	Sulphide-rich quartz near fold hinge	Fold hinge
NTH-HZR-02	Altered Gneiss	0.15	Weakly altered biotite gneiss	Distal alteration
NTH-QV-05	Quartz-Carbonate Vein	3.8	Brecciated vein with iron staining	Lithological contact

The highest gold grade (5.0 g/t) was obtained from a sulphide-rich quartz vein located at a fold hinge zone (Sample NTH-QV-04), highlighting the strong structural control on mineralization. Other notable results include 4.2 g/t Au from a massive milky quartz vein with visible sulphides at a dilational jog (NTH-QV-02) and 3.8 g/t Au from a brecciated quartz-carbonate vein at a lithological contact (NTH-QV-05). Altered host rocks yielded lower but still significant values (0.15-0.36 g/t),

consistent with a geochemical halo effect and potential lateral dispersion into the wall rock.

When categorized by vein type, Type 2 shear zone-hosted veins consistently yield the highest gold values (mean 3.33 g/t Au based on the samples in Table 1), confirming their economic significance. Type 1 foliation-parallel veins show moderate gold enrichment (mean 1.48 g/t Au), while altered wall rocks contain lower but anomalous gold values (mean 0.26 g/t Au).

Table 2. Gold Grades vs. Structural Settings

Structural Setting	Sample ID	Au (g/t)	Vein Type	Key Observations
Fold Hinge	NTH-QV-04	5	Type 2	Highest grade; sulphide-rich quartz vein
Dilational Jog (Shear Zone)	NTH-QV-02	4.2	Type 2	Massive quartz with visible sulphides
Lithological Contact	NTH-QV-05	3.8	Type 2	Brecciated vein at amphibolite-gneiss contact
Shear Zone (Foliation-Parallel)	NTH-QV-01	0.84	Type 1	Sheared vein with pyrite
Distal Alteration	NTH-HZR-02	0.15	N/A	Weakly altered biotite gneiss

4.5 Structural Architecture and Gold Distribution

Spatial analysis of gold assay data reveals systematic patterns of gold distribution in relation to structural features. The highest gold grades (>3 g/t Au) are consistently associated with quartz veins located at structural complexity zones, particularly fold hinges and dilational jogs along shear zones. Moderate gold grades (1-3 g/t Au) occur predominantly in shear zone-hosted and foliation-parallel veins, while lower grades (<1 g/t Au) characterize altered wall rocks and distal zones.

This pattern of gold distribution—with highest values in veins and decreasing concentrations in wall rocks—is typical of structurally controlled orogenic gold systems [28], [32]. The clear correlation between gold grades and specific structural settings provides compelling evidence for strong structural control on mineralization in the Nathenje area.

Brittle-ductile shear zones, commonly up to 2 m wide, play a central role in localizing mineralization. These zones exhibit a range of kinematic indicators including asymmetric boudins, drag folds, and quartz-feldspar segregation structures, consistent with a long-lived deformational history. Kinematic analysis based on S-C fabrics, rotated porphyroclasts, and asymmetric fold patterns indicates predominantly sinistral strike-slip to oblique-slip movement along NE-SW trending shear zones, likely reflecting transpressional deformation during the late stages of the Pan-African Orogeny.

Gold-bearing quartz veins are frequently localized at structurally favourable sites such as:

1. Dilational jogs along shear zones - These zones developed during fault movement, creating localized areas of extension where fluids could migrate and precipitate minerals.
2. Fold hinges, particularly in F_2 folds - The highest gold grade (5.0 g/t) was found in a sample from a fold hinge zone, highlighting these structures as premium targets.
3. Lithological boundaries between competent and incompetent units - Especially contacts between amphibolite and biotite gneiss, where mechanical contrast focused strain and fluid flow.
4. Zones of foliation deflection and strain localization - Areas where the regional fabric is disrupted by later deformation events.

These sites are often associated with alteration features and vein thickening, indicative of fluid

flowing and focusing along deformation-enhanced permeability pathways. The spatial correlation between high-grade gold samples and these structural features confirms the structural control on mineralization.

4.6. Deformation Timing and Gold Mineralization

The textural and structural relationships documented in this study, combined with the assay results, allow us to constrain the timing of gold mineralization relative to the deformation history of the area. The preferential occurrence of higher-grade mineralization in veins with orientations of the dominant foliation of $045^\circ/60^\circ\text{SE}$ supports the interpretation that gold emplacement occurred during progressive D2 transpressional deformation. Field evidence shows that the majority of high-grade gold samples are associated with NE-SW trending D2 shear zones. This suggests that D2 deformation played a critical role in focusing hydrothermal fluid flow and creating structural traps for gold deposition.

The three distinct generations of quartz veins identified in this study show varying gold contents, with the highest gold grades consistently associated with Type 2 shear zone-hosted veins. These veins display evidence of syn-tectonic emplacement (including folded banding and fractured appearances), suggesting that the main gold mineralization event occurred during the D2 transpressional phase (580-530 Ma).

The lower gold grades in the earlier foliation-parallel veins (Type 1) and minimal gold in the late extensional veins (Type 3) indicate that optimal conditions for gold mineralization were specifically linked to the D2 transpressional regime. This timing is consistent with the regional tectonic framework, corresponding to the late collisional to post-collisional stages of the Pan-African Orogeny in this part of the Mozambique Belt.

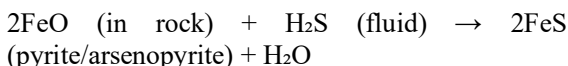
4.7. Lithological Controls and Fluid-Rock Interaction

While structural features clearly controlled the pathways for mineralizing fluids, our findings also indicate significant lithological influence on gold precipitation. The systematic occurrence of higher gold grades at contacts between amphibolite and biotite gneiss (Samples NTH-QV-04 and NTH-QV-05; 5.0 g/t and 3.8 g/t Au, respectively) suggests that chemical interaction between

hydrothermal fluids and wall rocks played an important role in gold deposition.

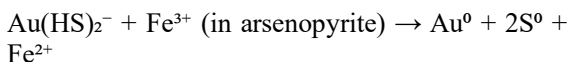
The intimate spatial relationship between gold and arsenopyrite at Nathenje reflects fundamental geochemical processes during ore formation. This chemical influence is further evidenced by the more intensive sulphide development observed where veins contact amphibolite compared to quartzo-feldspathic gneiss. The higher concentration of iron-bearing minerals in amphibolite likely promoted sulphide precipitation through wall-rock interaction with sulphur-bearing hydrothermal fluids, consequently triggering gold deposition. Gold deposition in Nathenje was likely driven by sulfidation reactions wherein arsenopyrite crystallization consumed reduced sulphur, destabilizing $\text{Au}(\text{HS})_2^-$ complexes [29]. This process was enhanced at amphibolite contacts, where Fe^{2+} from wall-rock alteration promoted arsenopyrite growth [33]. The resultant gold-arsenopyrite association mirrors global orogenic systems [34], reinforcing Nathenje's classification as a shear zone-hosted deposit.

Gold is primarily transported in orogenic systems as $\text{Au}(\text{HS})_2^-$ bisulphide complexes in moderately reduced, neutral-pH fluids [29]. These complexes remain stable at temperatures of 200–400°C and low oxygen fugacity, typical of mid-crustal shear zones. Arsenopyrite (FeAsS) plays a dual role in gold precipitation. Interaction with Fe-bearing host rocks (e.g., amphibolite) triggers sulfidation, consuming reduced sulphur (H_2S) from the fluid:



This then reduces sulphur activity, destabilizing $\text{Au}(\text{HS})_2^-$ and forcing gold precipitation [26]

Arsenopyrite's semiconducting properties create localized redox gradients. $\text{Au}(\text{HS})_2^-$ complexes adsorb onto arsenopyrite surfaces and reduce to native gold [27], [29]:



This interpretation is consistent with the observed spatial association between gold and sulphide minerals in the petrographic examination.

4.8. Comparison with Regional Orogenic Gold Systems

The structural controls on gold mineralization observed in the Nathenje area share several similarities with other orogenic gold systems worldwide, particularly those formed in high-grade

metamorphic terranes. The association of gold with transpressional structures, especially dilational jogs and fold hinges, parallels patterns documented in the Lupa Goldfield of Tanzania [35], parts of the Zimbabwe Craton [36], and the Paleoproterozoic Ashanti Belt in Ghana [37].

However, the Nathenje mineralization differs from many orogenic gold deposits in its high-grade metamorphic host rocks (upper amphibolite to granulite facies) and the important role of strain partitioning between contrasting lithologies. These characteristics more closely resemble gold systems in high-grade metamorphic terranes such as those in the Kerala region of southern India [38] and parts of the Nubian Shield in Sudan [39].

4.9. Exploration Implications and Gold Deposition

The geochemical and structural analysis provides clear targeting criteria for further exploration at Nathenje. These findings indicate that gold exploration should focus on:

1. NE-SW trending veins particularly where they intersect with competent amphibolite units
2. Structural complexity zones such as fold hinges and dilational jogs along shear zones
3. Lithological contacts between units with contrasting competence, especially between amphibolite and biotite gneiss
4. Zones exhibiting evidence of strain partitioning, which can create enhanced permeability networks.

This structural framework for gold mineralization in the Nathenje area is consistent with the characteristics of orogenic gold deposits elsewhere in the East African Orogen and provides a robust model for future exploration targeting.

5. Conclusions

This study elucidates the fundamental controls on orogenic gold mineralization within the high-grade metamorphic rocks of the Nathenje prospect through multiscale structural and geochemical analysis. Our integrated approach reveals that gold distribution is governed by a nested hierarchy of structural controls, from regional transpressional corridors to microscale sulphide grain boundaries, with the highest-grade mineralization (up to 5.0 g/t Au) systematically associated with zones of structural complexity.

The temporal framework established here demonstrates that gold emplacement occurred during syn-tectonic D_2 transpressional

deformation, as evidenced by the preferential orientation of high-grade veins slightly oblique to the regional foliation and their association with brittle-ductile shear zones. This timing relationship places mineralization during the late collisional stages of the Pan-African Orogeny (580–530 Ma), consistent with global patterns of orogenic gold formation.

Significantly, our results reveal that structural and chemical controls operated synergistically to localize gold precipitation. While transpressional structures provided the primary fluid pathways, lithological contrasts—particularly amphibolite-gneiss contacts—enhanced metal deposition through sulfidation reactions that destabilized gold-bearing hydrothermal complexes. The intimate spatial association between native gold and arsenopyrite reflects coupled precipitation processes typical of orogenic gold systems, wherein arsenopyrite crystallization triggered gold saturation through redox and pH modifications.

These findings establish Nathenje as a representative example of structurally controlled orogenic gold mineralization in high-grade metamorphic terranes and provide a robust exploration framework applicable throughout central Malawi's underexplored Precambrian basement. The hierarchical structural model developed here—emphasizing the intersection of regional shear zones with competent lithological units at sites of structural complexity—offers specific targeting criteria that could unlock Malawi's considerable but largely untapped gold potential. More broadly, this work contributes to our understanding of orogenic gold systems in high-grade metamorphic environments and demonstrates how detailed structural analysis can reveal the fundamental processes governing ore formation in complex polydeformed terranes. The systematic correlation between gold grades and specific structural-lithological settings provides insights applicable to similar Pan-African terranes throughout the East African Orogen and comparable high-grade metamorphic belts globally.

This study's interpretations are constrained by a relatively small sample size (10 rock samples, 7 fire assays) and limited spatial extent within the Nathenje prospect. Future investigations should expand to regional-scale sampling across central Malawi's basement terranes to test the broader applicability of these structural controls.

References

- [1] Dill, H. (2007). A review of mineral resources in Malawi: With special reference to aluminium variation in mineral deposits. *Journal of African Earth Sciences*, vol. 47, pp. 153–173, 2007, doi: 10.1016/j.jafrearsci.2006.12.006.
- [2] Chisambi, J., & von der Heyden, B. (2019). Primary gold mineralization in the Lisungwe valley area, Kirk range, southern Malawi. *South African Journal of Geology*, vol. 122, no. 4, pp. 505–518, 2019, doi: 10.25131/sajg.122.0039.
- [3] Chisambi, J., Haundi, T., & Tsokonombwe, G. (2020). Geologic structures associated with gold mineralization in the Kirk Range area in Southern Malawi. *Open Geosciences*, vol. 13, no. 1, pp. 1345–1357, 2021, doi: 10.1515/geo-2020-0304.
- [4] Chisambi, J., von der Heyden, B., & Tshibalanganda, M. (2020). Gold Exploration in Two and Three Dimensions: Improved and Correlative Insights from Microscopy and X-Ray Computed Tomography. *Minerals*, pp. 1–20.
- [5] Bloomfield, K., & Garson, M. (1965). The Geology of the Kirk Range-Lisungwe Valley Area. Bulletin No. 17., *The Government Printer, Zomba, Malawi*.
- [6] Malunga, G. (1992). Geochemical Exploration of Gold in the Likudzi Block, Geological Survey of Malawi. *Geological Survey of Malawi, unpublished report*.
- [7] Chisambi, J., & von der Heyden, B. (2023). The origin and evolution of the ore-forming fluids at the Manondo-Choma gold prospect, Kirk range, southern Malawi. *Open Geosciences*, vol. 15, no. 1, 2023, doi: 10.1515/geo-2022-0494.
- [8] Chisambi, J. & von der Heyden, B. (2019). Primary gold mineralization at Manondo – Choma area, Kirk range, Southern Malawi. *South African Journal of Geology*, no. 4.
- [9] Chisambi, J., Haundi, T., & von der Heyden, B. (2022). Aeromagnetic mapping of basement structures and gold mineralization characterization of Kirk range area, southern Malawi. *International Journal of Mining and Geo-Engineering*, vol. 56, no. 3, 2022, doi: 10.22059/IJMGE.2022.330117.594929.
- [10] Haundi, T., Tsokonombwe, G., Ghambi, S., Mkandawire, T., & Kasambara, A. (2021). An Investigation of the Socio-Economic Benefits of Small-Scale Gold Mining in Malawi. *Mining*, vol. 1, no. 1, 2021, doi: 10.3390/mining1010003.
- [11] Chisambi, J., Haundi, T., & Ghambi, S. (2023). Integrated interpretation of aeromagnetic and aeroradiometric data to delineate structures and hydrothermal alteration zones associated with Gold and Base metal Mineralization in Chitipa area, Northern Malawi. *International Journal of Mining and Geo-*

- Engineering*, vol. 57, no. 3, 2023, doi: 10.22059/IJMGE.2023.354353.595027.
- [12] Delvaux, D. *et al.*, (2018). Late Neoproterozoic (Pan-African) reactivations in the Mesoproterozoic Karagwe- Ankole Belt (KAB) in Kivu (RDC), Rwanda and Burundi: chronological framework and paleostress field. in *6th International Geologica Belgica meeting*.
- [13] Fritz, H. *et al.*, (2013). Journal of African Earth Sciences Orogen styles in the East African Orogen: A review of the Neoproterozoic to Cambrian tectonic evolution. *Journal of African Earth Sciences*, vol. 86, pp. 65–106, doi: 10.1016/j.jafrearsci.2013.06.004.
- [14] Stern, R. J. (2002). Crustal evolution in the East African Orogen: a neodymium isotopic perspective, vol. 34, pp. 109–117, 2002.
- [15] Bloomfield, K., & Garson, M. (1965). The Geology of the Kirk Range-Lisungwe Valley Area. Ministry of Natural Resources. Geological Survey Department. Bulletin No.17., *The Government Printer; Zomba. Malawi*, 1965.
- [16] Kroner, A., & Collins, A. (2001). The East African Orogen: New Zircon and Nd Ages and Implications for Rodinia and Gondwana Supercontinent Formation and Dispersal. *Gondwana Research*, no. 2, pp. 179–181, 2001.
- [17] Sommer, H., & Kröner, A. (2013). Ultra-high temperature granulite-facies metamorphic rocks from the Mozambique belt of SW Tanzania. *Lithos*, vol. 170–171, pp. 117–143, 2013, doi: 10.1016/j.lithos.2013.02.014.
- [18] Ring, U., Kröner, A., & Toulkeridis, T. (1997). Palaeoproterozoic granulite-facies meta-morphism and granitoid intrusions in the Ubendian-Usagaran Orogen of northern Malawi, east-central Africa. *Precambrian Reserch.*, vol. 85, 27–51.
- [19] Bjerkgaard, T., & Stein, H. (2008). The Niassa Gold Belt , northern Mozambique – A segment of a continental-scale Pan-African gold-bearing structure ?. *Journal of African Earth Sciences*, vol. 53, no. 1–2, pp. 45–58, 2009, doi: 10.1016/j.jafrearsci.2008.09.003.
- [20] Bingen *et al.*, (2009). “Geochronology of the Precambrian crust in the Mozambique belt in NE Mozambique , and implications for Gondwana assembly. *Precambrian Res*, vol. 170, pp. 231–255, 2009, doi: 10.1016/j.precamres.2009.01.005.
- [21] Boyd *et al.*, (2010). The Geology and Geochemistry of the East African Orogen In Northeastern Mozambique. *Geological Society of South Africa*, vol. 113, pp. 87–129, 2010, doi: 10.2113/gssajg.113.1.87.
- [22] Macey *et al.*, (2010). Mesoproterozoic geology of the Nampula Block , northern Mozambique : Tracing fragments of Mesoproterozoic crust in the heart of Gondwana. *Precambrian Research*. vol. 182, pp. 124–148, 2010, doi: 10.1016/j.precamres.2010.07.005.
- [23] Ring, U & Kronner, A. (2002). Shear-zone patterns and eclogite-facies metamorphism in the Mozambique belt of northern Malawi , east-central Africa : implications for the assembly of Gondwana. *Precambrian Res*, vol. 116, pp. 19–56.
- [24] Cardozo, N., & Allmendinger, R. (2013). Spherical projections with OSX Stereonet. *Computer and Geosciences*, vol. 51, 2013, doi: 10.1016/j.cageo.2012.07.021.
- [25] Allmendinger, R. (2011). Stereonet 7,” *Distribution*.
- [26] Goldfarb, R., & Groves, D. (2015). Orogenic gold: Common or evolving fluid and metal sources through time. *Lithos*, vol. 233, pp. 2–26, 2015, doi: 10.1016/j.lithos.2015.07.011.
- [27] Goldfarb, R., & Groves, D. (2015). Orogenic gold: Common or evolving fluid and metal sources through time. *Lithos*, vol. 233, pp. 2–26, 2015, doi: 10.1016/j.lithos.2015.07.011.
- [28] Goldfarb, R., Groves, D., & Gardoll, S. (2001). Orogenic gold and geologic time : a global synthesis. *Ore Geol Rev*.
- [29] Aliyari, F., Rastad, E., Goldfarb, R., & Abdollahi, J. (2014). Geochemistry of hydrothermal alteration at the Qolqoleh gold deposit , northern Sanandaj – Sirjan metamorphic belt , northwestern Iran : Vectors to high-grade ore bodies. *J Geochem Explor*, vol. 140, pp. 111–125, 2014, doi: 10.1016/j.gexplo.2014.01.007.
- [30] Large, D., & Walcher, E. (1999). The Rammelsberg massive sulphide Cu-Zn-Pb-Ba-Deposit, Germany: an example of sediment-hosted, massive sulphide mineralization. *Springer*, vol. 34, no. 5–6, pp. 522–538, Jul. 1999, doi: 10.1007/s001260050218.
- [31] Tombros, S., & Liu, J. (2014). “Origin of a barite-sulphide ore deposit in the Mykonos intrusion , cyclades : Trace element , isotopic , fluid inclusion and raman spectroscopy evidence. *Ore Geol Rev*, vol. 67, pp. 139–157, 2015, doi: 10.1016/j.oregeorev.2014.11.016.
- [32] Nykänen, V., Groves, D., & Gardoll, S. (2008). Reconnaissance-scale conceptual fuzzy-logic prospectivity modelling for iron oxide copper – gold deposits in the northern Fennoscandian Shield, Finland. *Australian Journal of Earth Sciences*, vol. 55, no. 1, pp. 25–38, Feb. 2008, doi: 10.1080/08120090701581372.
- [33] Phillips, G., & Powell, R. (2012). Origin of Witwatersrand gold: A metamorphic devolatilisation-hydrothermal replacement model. *Transactions of the Institutions of Mining and Metallurgy, Section B: Applied Earth Science*, vol. 120, no. 3, 2012, doi: 10.1179/1743275812Y.0000000005.

- [34] Hastie, E., Kontak, D., & Lafrance, B. (2020). Gold Remobilization: Insights from Gold Deposits in the Archean Swayze Greenstone Belt, Abitibi Subprovince, Canada. *Economic Geology*, vol. 115, no. 2, 2020, doi: 10.5382/econgeo.4709.
- [35] Kwelwa, S., Dirks, P., Sanislav, I., Blenkinsop, T., & Kolling, S. (2018). Archean gold mineralization in an extensional setting: The structural history of the Kukuluma and Matandani deposits, Geita Greenstone Belt, Tanzania. *Minerals*, vol. 8, no. 4, 2018, doi: 10.3390/min8040171.
- [36] Austin, J., & Blenkinsop, T. (2007). The Cloncurry Lineament: Geophysical and geological evidence for a deep crustal structure in the Eastern Succession of the Mount Isa Inlier. *Precambrian Res*, vol. 163, no. 1–2, pp. 50–68, 2008, doi: 10.1016/j.precamres.2007.08.012.
- [37] Li, Y., (2015). Zircon geochronology , geochemistry and stable isotopes of the Wang ' ershan gold deposit , Jiaodong Peninsula , China. *J Asian Earth Sci*, vol. 113, pp. 695–710, 2015, doi: 10.1016/j.jseaes.2015.03.036
- [38] Santosh, M., Wilde, S., & Li, J. (2007). Timing of Paleoproterozoic ultrahigh-temperature metamorphism in the North China Craton: Evidence from SHRIMP U – Pb zircon geochronology. *Precambrian Res*, vol. 159, pp. 178–196, 2007, doi: 10.1016/j.precamres.2007.06.006.
- [39]. Ganguly *et al.*, (2016). Geochemical characteristics of gold bearing boninites and banded iron formations from Shimoga greenstone belt , India : Implications for gold genesis and hydrothermal processes in diverse tectonic settings. *Ore Geol Rev*, vol. 73, pp. 59–82, doi: 10.1016/j.oregeorev.2015.10.013.



دانشگاه صنعتی شاهرود

نشریه مهندسی معدن و محیط زیست

www.jme.shahroodut.ac.ir نشانی نشریه:



انجمن مهندسی معدن ایران

کنترل‌های ساختاری بر کانی‌سازی طلای کوه‌زایی در سنگ‌های دگرگونی درجه بالا: بینش‌هایی از منطقه اکتشافی ناتنجه، مالاوی مرکزی

جاشوا چیسامبی^{۱*}، لئونارد کالیندکافه^۲، کتی ماگوازا^۲، روث مومبا^۲ و مارتین کامزا^۲

۱. دپارتمان مهندسی معدن، دانشگاه بازرگانی و علوم کاربردی مالاوی، بلانتایر، مالاوی

۲. شرکت سرمایه‌گذاری معدن مالاوی (MAMICO)، لیلونگوه، مالاوی

اطلاعات مقاله	چکیده
تاریخ ارسال: ۲۰۲۵/۰۶/۰۵	<p>منطقه ناتنجه در مرکز مالاوی میزبان کانی‌سازی طلای قابل توجهی در سنگ‌های دگرگونی درجه بالای کمربند موزامبیک است، اما با وجود فعالیت‌های گسترده معدنکاری دستی، همچنان ناشناخته باقی مانده است. کنترل‌های ساختاری بر کانی‌سازی طلای سنگ بستر اولیه در این سنگ‌های دگرگونی درجه بالا هنوز به خوبی درک نشده‌اند و اکتشاف سیستماتیک و توسعه منابع را محدود می‌کنند. ما نقشه‌برداری میدانی یکپارچه، تجزیه و تحلیل ساختاری، بررسی پتروگرافی و نمونه‌برداری ژئوشیمیایی را برای توصیف کنترل‌های کانی‌سازی طلا در منطقه اکتشافی ناتنجه، مرکز مالاوی انجام دادیم. اندازه‌گیری‌های ساختاری دقیق همراه با تجزیه و تحلیل استریوگرافی، سه مرحله تغییر شکل را نشان می‌دهد که کانی‌سازی طلا عمدتاً با ساختارهای ترفاشاری D₂ مرتبط است. نتایج سنجش آتش، غلظت‌های قابل توجهی از طلا (۰.۱۵-۵.۰ گرم در تن طلا) را در رگه‌های کوارتز حاوی آرسنوپیریت نشان می‌دهد که بالاترین عیارها به طور سیستماتیک در مناطق پیچیدگی ساختاری رخ می‌دهند. تجزیه و تحلیل پتروگرافی، ذرات طلای بومی (۵-۵۰ میکرومتر) را نشان می‌دهد که به طور نزدیکی با آرسنوپیریت در امتداد مرزهای دانه و درون ریزشکستگی‌ها مرتبط هستند که نشان‌دهنده فرآیندهای بارش همراه است. نکته مهم این است که ما یک سیستم کنترل ساختاری سلسله مراتبی را شناسایی می‌کنیم که از زون‌های برشی منطقه‌ای با روند شمال شرقی-جنوب غربی تا مرزهای سولفیدی در مقیاس میکرو، با لولاهای چین‌خوردگی، جاگ‌های رقیق‌شدگی و تماس‌های آمفیبولیت-گنیس عمل می‌کند و عیار طلای بالاتری (بیش از ۳ گرم در تن طلا) نسبت به سایر محیط‌های ساختاری ارائه می‌دهد. نتایج ما اولین مدل ساختاری جامع برای کانی‌سازی طلا در ناحیه دگرگونی مرکز مالاوی را ایجاد می‌کند و معیارهای هدف‌گیری خاصی را برای محیط‌های دگرگونی مشابه با عیار بالا در سراسر کوه‌زایی شرق آفریقا ارائه می‌دهد.</p>
تاریخ داوری: ۲۰۲۵/۰۷/۳۰	
تاریخ پذیرش: ۲۰۲۵/۰۸/۲۹	
DOI: 10.22044/jme.2025.16348.3183	
کلمات کلیدی	
طلای کوه‌زایی	
کنترل ساختاری	
زون‌های برشی	
لوله‌های چین‌خوردگی	
مجموع زیرزمین مالاوی	